

Terahertz generation from laser-driven ultrafast current propagation along a wire target

H. B. Zhuo,^{1,2,*} S. J. Zhang,¹ X. H. Li,¹ H. Y. Zhou,¹ X. Z. Li,¹ D. B. Zou,¹ M. Y. Yu,³
H. C. Wu,^{2,3} Z. M. Sheng,^{2,4,5} and C. T. Zhou^{1,6}

¹College of Science, National University of Defense Technology, Changsha 410073, People's Republic of China

²IFSA Collaborative Innovation Center, Shanghai Jiao Tong University, Shanghai 200240, People's Republic of China

³Institute for Fusion Theory and Simulation and Department of Physics, Zhejiang University, Hangzhou 310027, People's Republic of China

⁴SUPA, Department of Physics, University of Strathclyde, Glasgow G4 0NG, United Kingdom

⁵Key Laboratory for Laser Plasmas (MoE) and Department of Physics and Astronomy, Shanghai Jiao Tong University, Shanghai 200240, People's Republic of China

⁶Institute of Applied Physics and Computational Mathematics, Beijing 100094, People's Republic of China

(Received 1 August 2016; published 5 January 2017)

Generation of intense coherent THz radiation by obliquely incidenting an intense laser pulse on a wire target is studied using particle-in-cell simulation. The laser-accelerated fast electrons are confined and guided along the surface of the wire, which then acts like a current-carrying line antenna and under appropriate conditions can emit electromagnetic radiation in the THz regime. For a driving laser intensity $\sim 3 \times 10^{18}$ W/cm² and pulse duration ~ 10 fs, a transient current above 10 KA is produced on the wire surface. The emission-cone angle of the resulting ~ 0.15 mJ (~ 58 GV/m peak electric field) THz radiation is $\sim 30^\circ$. The conversion efficiency of laser-to-THz energy is $\sim 0.75\%$. A simple analytical model that well reproduces the simulated result is presented.

DOI: 10.1103/PhysRevE.95.013201

Interaction of high-power laser pulses with solid targets is usually accompanied by the generation of a significant number of energetic electrons. The latter can produce secondary effects such as bright x- and γ -ray emission [1], ion acceleration [2,3], etc. [4–6], which have many practical applications. Recently, there has been much interest on the generation of intense THz radiation from laser-plasma interaction [7–11]. Unlike the crystal-based THz sources, the latter is not severely limited by material damage. One can thus expect that tabletop sources of THz radiation approaching the millijoule level can be realized. In fact, efficient THz radiation generation has been demonstrated in experiments where thin metal foils are irradiated by ultrashort intense laser pulses [12–14]. Two major mechanisms have been proposed to explain the experimental results. One is coherent transition radiation [12], which can take place when the laser-accelerated electrons reaching the rear surface of the target pass through the interface between the target and vacuum. The other is target normal sheath radiation [13,14], which can occur when the electrons are decelerated by the intense electrostatic sheath field on the rear target surface. In both cases the radiation is closely associated with the transient dynamics of the laser-accelerated electrons arriving at the target rear side, and its power is limited by the large angular divergence and therefore rapid decrease of the fast-electron density.

A number of novel phenomena have been observed in relativistic laser interaction with wire targets [15–19]. Collimation and guidance of energetic electrons with energies at the few hundred KeV to MeV level have been demonstrated [15,18,19]. Field propagation at light speed along a wire has been observed and the induced transient current can be up to $\sim 10^4$ A [17]. It has been suggested that balance of the radial electric and azimuthal magnetic field forces at the wire surface results in a fine collimation of the electrons [15,20,21].

In this paper, we propose a simple method for producing intense THz waves by laser-wire interaction. As illustrated in Fig. 1(a), we consider an intense laser pulse obliquely shining on the center of a wire target. As the laser-accelerated fast electrons are self-collimated and guided along the wire, a huge transient current is formed on the wire surface. Considering that the temporal profile of this current follows roughly that of the laser pulse (typically a few fs or more for TW lasers), one can see that the pulse envelope corresponds to a carrier frequency of $\sim 10^{13}$ Hz. The interaction is therefore be considered as a natural coherent source of THz radiation, with the current-carrying wire acting as a line antenna.

To demonstrate the operation of the proposed THz radiation source, a series of two-dimensional (2D) simulations were carried out using the particle-in-cell (PIC) code PDLPICC2D [22,23]. In the simulations, a *p*-polarized laser pulse incidents on the center of the wire target at a 30° angle. The laser intensity is 3.08×10^{18} W/cm², corresponding to the laser parameter $a_0 = eE/m_e\omega_0c = 1.5$, where m_e is electron mass, c is the speed of light, and ω_0 is laser frequency. The laser pulse is Gaussian in the *y* direction with (full width at half maximum) spot size $w_0 = 6\lambda_0$, where $\lambda_0 = 1.0 \mu\text{m}$ is the laser wavelength. Its time profile is $\exp(-t^2/2\tau_0^2)$ with $\tau_0 = 3T_0$, where T_0 is laser period. The length of the wire is $L = 30\lambda_0$ and its thickness is $D = 2.0\lambda_0$. The simulation box is $100\lambda_0 \times 100\lambda_0$ with a spatial resolution up to 100 cells per wavelength. Each cell contains 100 ions and 100 electrons. The target is assumed to be fully ionized and the electron density is $n_0 = 1.12 \times 10^{21} \text{cm}^{-3}$, or $10n_c$, where n_c is the critical density. For the simulation time of interest, the ions can be assumed to be fixed. In order to resolve the Debye length of the plasma, the initial electron temperature is taken to be 1 keV.

The distinctive pattern of the radiation produced from the laser-wire interaction is shown in Fig. 2. Two spherical wave fronts, one centered at the center of the wire and the other centered at the right end of the wire, can be clearly observed.

*hongbin.zhuo@gmail.com

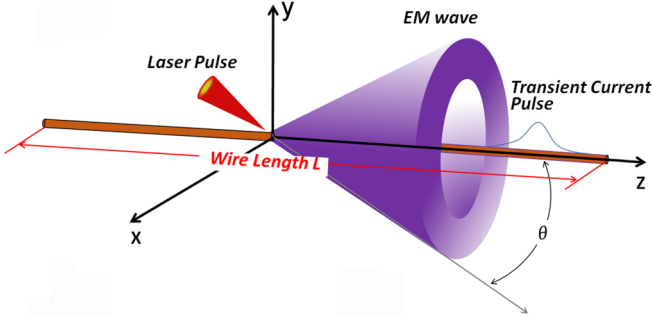


FIG. 1. The proposed scheme for THz-radiation generation. The laser-wire interaction at the center of the wire results in an intense transient current pulse that propagates along the wire to its right end. The wire is along the z axis and θ is the observation angle.

The first spherical wave is produced when the laser pulse acts on the center of the wire and accelerates the electrons there. The second spherical wave is generated when the hot electrons propagating stably along the wire reach the right end of the wire. The two spherical light waves then propagate away from their sources with the corresponding Poynting vectors predominantly normal to the spherical wave fronts. However, the intensity of radiation depends on the emission angle and is thus not distributed uniformly over the wave front. These characteristics are quite similar to that of the radiation from a line antenna driven by a current pulse [25].

For large-angle incidence of laser pulse on a wire target, the electron acceleration mechanism is similar to that given in Refs. [20,21]. As can be seen in Figs. 3(a), 3(b), except for the few electrons that escape from the target, most of the laser-accelerated electrons are propagating along the wire with good collimation. Figures 3(c)–3(f) indicate that the latter can

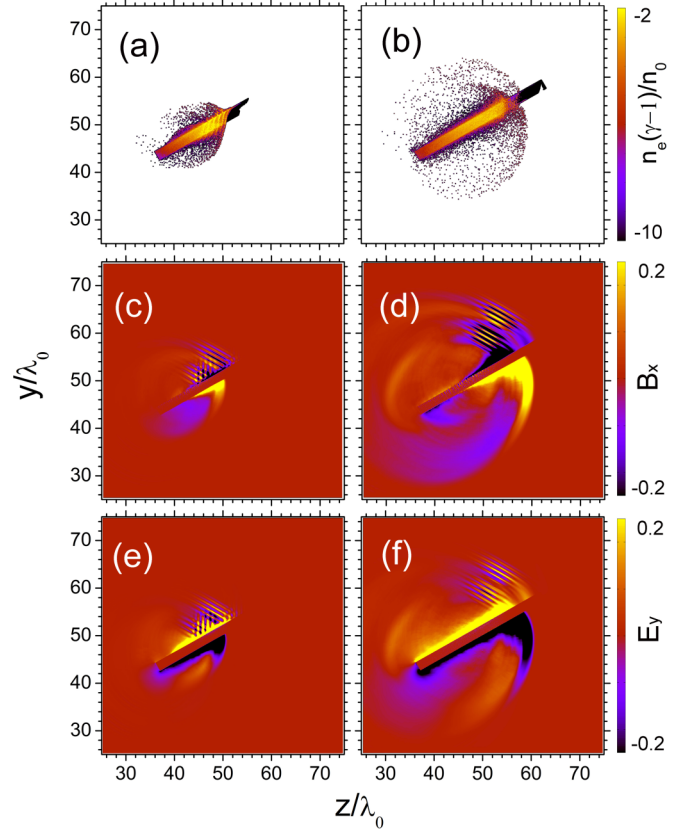


FIG. 3. The electron kinetic energy density (a) and (b), the self-generated surface magnetic field B_x (c) and (d), and the electric field E_y (e) and (f), at $t = 55T_0$ (left column), $65T_0$ (right column), respectively.

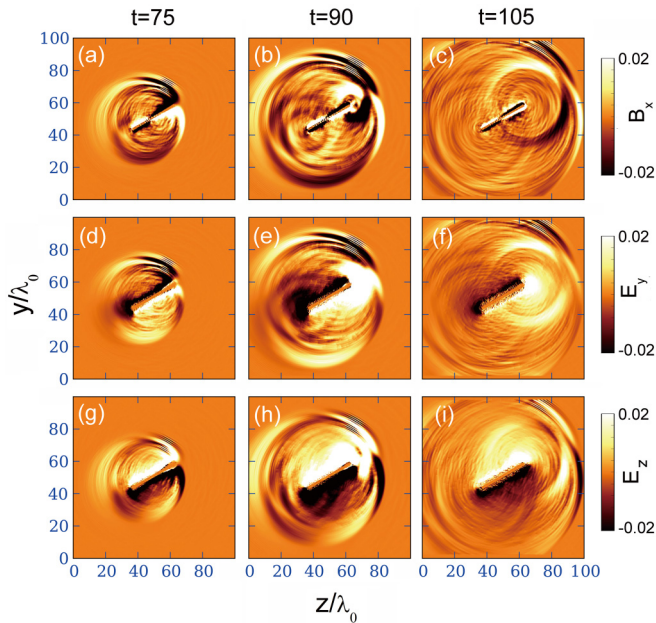


FIG. 2. Snapshots of the radiation field components B_x , E_y , and E_z at three different times. Here and in the following figures, \mathbf{E} and \mathbf{B} are normalized by $m_e \omega_0 c / e$.

be attributed to the surface fields on the wire: the intense radial electric field E_y , induced by the charge-separation field of the escaped high-density MeV electrons, tends to pull the electrons back to the surface. However, the current induces an intense azimuthal magnetic field B_x of the order of a few hundred MG, which tends to push the electrons away from the surface. A balance of the electric eE_y and magnetic $(e/c)v_e \times \mathbf{B}$ forces results in collimation and confinement of the fast electrons, which propagates at nearly the light speed. Additional simulations show that when the incidence angle of the laser is reduced, collimation of the fast electrons rapidly weakens and the radiation power rapidly decreases.

The total number of laser-accelerated hot electrons can be estimated from the energy balance relation $N_{\text{total}} = fE(k_B T_h)^{-1}$, where f is the fraction of laser energy absorbed by hot electrons, E is the pulse energy, and $k_B T_h$ is the hot electron temperature as predicted by the ponderomotive scaling [24]. For $f \sim 10\%$, $E \sim 20$ mJ, and $k_B T_h \sim 0.2$ MeV, as obtained from the simulation, the total number of hot electrons at the laser focus is about 6×10^{10} . The current formed on the wire surface can be roughly estimated from the surface magnetic field strength as $I \approx \pi B_x D / \mu_0$, or $\sim 1.1 \times 10^4$ A, for $B_x \approx 0.2 m_e \omega_0 c / e \sim 2200$ Tesla at $t = 65T_0$, as given in Fig. 3. The number of electrons in the transient current can be calculated by integrating the current over the pulse duration. It is about $\sim 1.72 \times 10^9$, which is far

less than the total number of laser-accelerated electrons. This shows that only the fastest electrons, typically the suprathermal ones in the Maxwellian distribution, contribute to the transient current. The slower electrons are driven back to the wire by the space-charge force and neutralized by the wire plasma.

In the following, the Smith antenna model [25] is used to analyze the simulation results. We assume that a transient current is formed at $z = 0$ and propagating along the wire to the right end of the target. We neglect the temporal variance of the current profile during the short propagation process and assume that the speed of the current is c . Thus, the transient currents induced on the wire surface is then $I(z, t) = I_s(t - z/c)$, where $I_s(t) = I_0 e^{-t^2/2\tau_0^2}$ is the initial temporal profile, where I_0 is peak current intensity. As $r/L \rightarrow \infty$, where r is the distance to the observer, the radiation electric field of the moving current source is given by the Smith's model as [25]

$$\vec{E}(\vec{r}, t) = \frac{\mu_0 c \sin \theta}{4\pi r(1 - \cos \theta)} \{I_s(t - r/c) - I_s(t - r/c - \tau_d)\} \hat{\theta}, \quad (1)$$

where θ is observation angle with respect to the wire direction, and $\tau_d = \frac{L}{2c}(1 - \cos \theta)$ is the retarded time between the source and terminal. Equation (1) then leads to the spectral intensity of the radiation

$$\frac{d^2 W}{d\Omega d\omega} = \frac{\mu_0 c I_0^2 \tau_0^2 \sin^2 \theta}{4\pi(1 - \cos \theta)^2} \sin^2 \frac{\omega \tau_d}{2} e^{-\tau_0^2 \omega^2}. \quad (2)$$

After integrating (2) over the frequency, we obtain the radiation energy into the solid angle as

$$\frac{dW}{d\Omega} = \frac{\mu_0 c I_0^2 \tau_0 \sin^2 \theta}{16\sqrt{\pi}(1 - \cos \theta)^2} (1 - e^{-\tau_d^2/4\tau_0^2}). \quad (3)$$

Integrating Eq. (3) over the solid angle Ω , one can obtain the total energy radiated from the wire:

$$W = \frac{\mu_0 c I_0^2 \tau_0}{4\sqrt{\pi}} \left[\gamma - 2 + \ln \alpha^2 + \frac{\sqrt{\pi}}{\alpha} \text{Erf}(\alpha) + E_1(\alpha^2) \right], \quad (4)$$

where $\alpha = \frac{L}{2c\tau_0}$, $\gamma = 0.57721$ is Euler's constant, Erf is the error function, and E_1 is the exponential integral.

Figure 4(a) shows the radiation electric field E_θ obtained from Eq. (1). The parameters are the same as Fig. 2. We see that the spherical wave fronts are centered at the center and right end of the wire. This is to be expected since the first term in Eq. (1) involves only r and the time delay $t - r/c$, so that it corresponds to the spherical wave centered at the source at $z = 0$. The second term in Eq. (1) involves the radial distance r from the wire end and the time delay $t - r/c - \tau_d$, so that it corresponds to the spherical wave centered at $z = L/2$. An analogy can be drawn between the radiation from this pulse-excited line antenna and that from a negative moving point charge. When the electron pulse leaves the source, spherical radiation with negative electric field is produced. This is analogous to a point charge undergoing acceleration in the direction of its velocity. As the electron pulse moves along the wire, no radiation is produced, which is analogous to a point charge moving at constant velocity. When the electron pulse reaches the end of the wire, spherical radiation with positive electric field is generated. This is analogous to a point charge undergoing deceleration in the direction of its velocity.

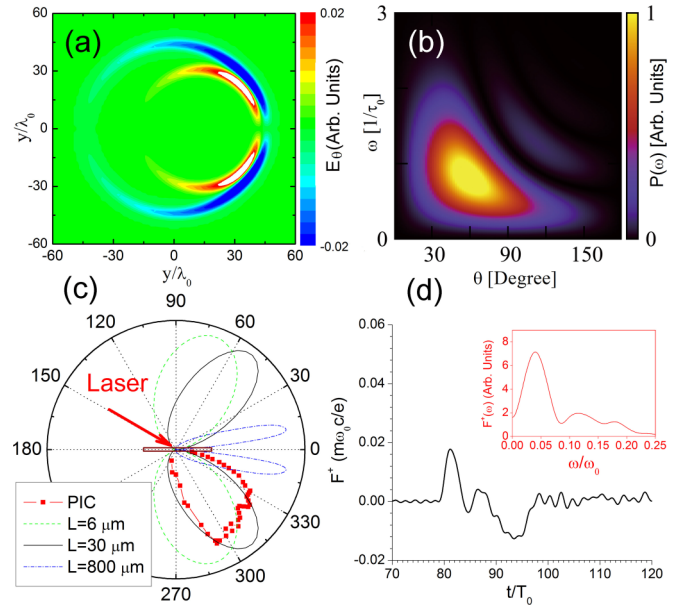


FIG. 4. Results from the simple analytical model: (a) E_θ at $t = 50T_0$, (b) radiation spectrum vs the observation angle θ , and (c) angular distribution of the radiation energy for different wire lengths. (d) Temporal profile of the radiation and its spectrum (inset) from the simulation. In (c), the radiation energy from the simulation is indicated by the solid squares, which are fitted to the curves for $L = 30 \mu\text{m}$ for comparison. Note: because of the huge difference in the radiated energies, the curves for $L = 6 \mu\text{m}$ and $L = 800 \mu\text{m}$ have been magnified by factors of 3 and $1/80$, respectively.

Thus, similar to that of bremsstrahlung, the radiation vanishes for $\theta = 0^\circ$.

Figure 4(b) shows the power spectrum of the radiation as obtained from Eq. (2). The optimal angle of the radiation is around $\theta = 57^\circ$, where the spectrum is peaked around $\omega \sim 0.8/\tau_0 = 12.6 \text{ THz}$, which is roughly the carrier frequency of the driving laser pulse. At larger angles of observation, the peak of the spectrum shifts to lower frequencies and its width decreases.

Figure 4(c) shows the angular distribution of the radiation energy as obtained from Eq. (3) for different wire lengths. One sees that the radiation from a short wire is rather weak, and it peaks closer to the normal (to the wire) direction. With increasing wire length, the angular distribution of the THz energy is tipped forward towards the direction of the wire, together with sharper and more intense peaks. This behavior is similar to that of radiation from a traveling-wave antenna with time-harmonic excitation, where the angle of the radiation shifts to the forward direction and its main lobe narrows as the electrical length of the antenna is increased [26]. For comparison, the time integral of the radiation flux vs. the observation angle, as obtained from the simulation, is also shown in Fig. 4(c). We see that, except for the profile of the maximum-intensity region (probably due to nonlinear effects), there is good fit with the curve for $L = 30 \mu\text{m}$.

The temporal profile of the radiation flux $F^+ = (E_y - cB_x)/2$ at $\theta = 30^\circ$ from our simulation is shown in Fig. 4(d). The peak amplitude is over $0.018 m_e \omega_0 c/e$, corresponding to an electric field strength of over 58 GV/m . Integrated over the

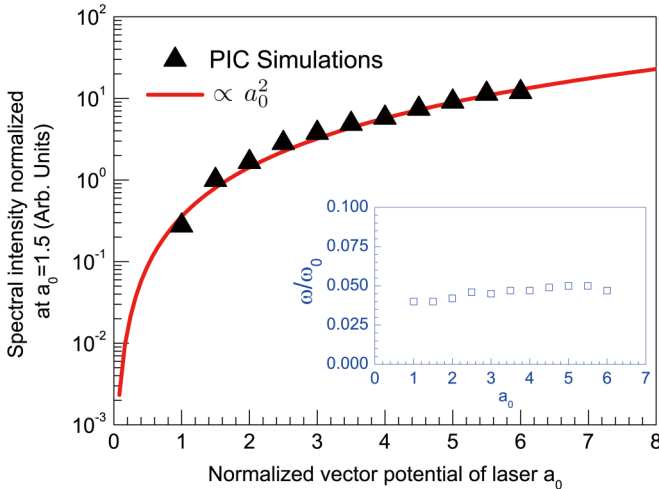


FIG. 5. Parametric dependence of the radiation intensity for $\theta = 30^\circ$ and the central frequency (inset) as a function of the laser intensity. The solid curve is from the model, and the solid triangles and hollow squares are PIC simulation results.

emission cone angle $\Omega \sim 30^\circ$ and duration $\sim 20T_0$ (i.e., 66 fs), the total radiation energy is about ~ 0.15 mJ, corresponding to a laser-to-THz radiation conversion efficiency of over 0.75%. Using this radiation energy in Eq. (4), the driven current is ~ 10 KA, which is fairly consistent with our estimate. The central frequency of the emission is $\omega = 0.04\omega_0$ (see the inset), which is somewhat less than that of the model prediction $\omega = 0.05\omega_0$. This can be attributed to nonlinear modification of the electron-bunch profile during its propagation along the wire target, which can result in deformation of the second half cycle of the wave.

From Eq. (3) we see that the radiation power is proportional to the square of the current intensity, which is determined by the laser intensity and the laser-to-fast-electrons conversion efficiency. Under the parameters of our simulation, the ponderomotive force is dominant for the hot electron generation, and the current is proportional to the total number of electrons accelerated by the laser. Thus, the radiation power satisfies $P \propto a_0^2$, which fits well with our simulation results, as shown in Fig. 5. Moreover, as we can see, the center frequency of the radiation is almost independent with the laser intensities (shown in the inset). This is consistent with our assumption that only the fast hot electrons contribute to the radiation.

In practice, it is often necessary to apply the intense THz radiation relatively far away from the source. According to Eq. (3) of the metal-wire antenna model, in the limit $L \rightarrow \infty$ the radiation angle becomes $\theta \rightarrow 0$. That is, the radiation appears as a surface wave propagating along the wire surface. The wave intensity will, however, be limited by resistive heating of the transient current and ionization of the wire surface by the propagating surface wave. On the other hand, theoretical and experimental results have shown that metal wires can serve as excellent low-loss and low-dispersion waveguides for Sommerfeld waves in the gigahertz-to-THz frequency range [27,28].

It should also be emphasized that the present scheme for THz radiation depends strongly on the requirement that the driving laser pulse be of sufficiently high contrast and shot duration. A laser with too-long duration or too-intense prepulse can lead to strong heating and expansion, and thus destruction, of the wire plasma. However, current short-pulse lasers and techniques [29], such as using a plasma mirror to achieve ultrahigh pulse-to-prepulse contrast ratio are now available for carrying out the proposed scheme in experiments.

In summary, we have proposed a simple tabletop scheme for producing the intense coherent THz radiation by obliquely incidenting an intense laser pulse on a wire target. The fast electrons generated by the laser-plasma interaction on the wire surface are self-confined and propagate along the wire as a short pulse. The scenario is somewhat similar to a line antenna. It is found that intense THz radiation having electric field > 58 GV/m and laser-to-THz radiation conversion efficiency up to 0.75% can be achieved. A simple analytical model is also given, the obtained angular distribution and energy spectrum of the radiation are in fairly good agreement with that from the 2D PIC simulations. Our scheme therefore offers a relatively simple route for producing ultrastrong THz radiation for practical applications. Moreover, the efficient self-confined long-distance transport of a dense energetic electron bunch along the surface of a wire, a crucial ingredient of the present scheme, can also be potentially useful for other schemes and applications in high-energy density physics research.

This work is supported by the National Basic Research Program of China (Grant No. 2013CBA01504), the Science Challenge Project (JCKY2016212A505), and the National Natural Science Foundation of China (Grants No. 11475259, No. 11175253, No. 11374262, and No. 91230205). We would like to thank the Guangzhou National Supercomputing Center for providing their computing facilities.

- [1] K. W. D. Ledingham, I. Spencer, T. McCanny, R. P. Singal, M. I. K. Santala, E. Clark, I. Watts, F. N. Beg, M. Zepf, K. Krushelnick, M. Tatarakis, A. E. Dangor, P. A. Norreys, R. Allott, D. Neely, R. J. Clarke, A. C. Machacek, J. S. Wark, A. J. Cresswell, D. C. W. Sanderson, and J. Magill, *Phys. Rev. Lett.* **84**, 899 (2000).
- [2] E. L. Clark, K. Krushelnick, J. R. Davies, M. Zepf, M. Tatarakis, F. N. Beg, A. Machacek, P. A. Norreys, M. I. K. Santala, I. Watts, and A. E. Dangor, *Phys. Rev. Lett.* **84**, 670 (2000).

- [3] H. B. Zhuo, Z. L. Chen, W. Yu, Z. M. Sheng, M. Y. Yu, Z. Jin, and R. Kodama, *Phys. Rev. Lett.* **105**, 065003 (2010).
- [4] Z. Jin, Z. L. Chen, H. B. Zhuo, A. Kon, M. Nakatsutsumi, H. B. Wang, B. H. Zhang, Y. Q. Gu, Y. C. Wu, B. Zhu, L. Wang, M. Y. Yu, Z. M. Sheng, and R. Kodama, *Phys. Rev. Lett.* **107**, 265003 (2011).
- [5] S. J. Zhang, H. B. Zhuo, D. B. Zou, L. F. Gan, H. Y. Zhou, X. Z. Li, M. Y. Yu, and W. Yu, *Phys. Rev. E* **93**, 053206 (2016).

- [6] H. B. Zhuo, Z. Jin, M. Y. Yu, Z. M. Sheng, H. Xu, Y. Y. Ma, Y. Yin, F. Q. Shao, W. M. Zhou, and R. Kodama, *Phys. Plasmas*, **19**, 043108 (2012).
- [7] H. Hamster, A. Sullivan, S. Gordon, W. White, and R. W. Falcone, *Phys. Rev. Lett.* **71**, 2725 (1993).
- [8] H. Hamster, A. Sullivan, S. Gordon, and R. W. Falcone, *Phys. Rev. E* **49**, 671 (1994).
- [9] A. Sagisaka, H. Daido, S. Nashima, S. Orimo, K. Ogura, M. Mori, A. Yogo, J. Ma, I. Daito, A. S. Pirozhkov, S. V. Bulanov, T. Z. Esirkepov, K. Shimizu, H. Hosoda *et al.*, *Appl. Phys. B* **90**, 373 (2008).
- [10] Y. T. Li *et al.*, *Appl. Phys. Lett.* **100**, 254101 (2012).
- [11] G. Q. Liao, Y. T. Li, C. Li, L. N. Su, Y. Zheng, M. Liu, W. M. Wang, Z. D. Hu, W. C. Yan, J. Dunn, J. Nilsen, J. Hunter, Y. Liu, X. Wang, L. M. Chen, J. L. Ma, X. Lu, Z. Jin, R. Kodama, Z. M. Sheng, and J. Zhang, *Phys. Rev. Lett.* **114**, 255001 (2015).
- [12] G.-Q. Liao, Y.-T. Li, Y.-H. Zhang, H. Liu, X.-L. Ge, S. Yang, W.-Q. Wei, X.-H. Yuan, Y.-Q. Deng, B.-J. Zhu, Z. Zhang, W.-M. Wang, Z.-M. Sheng, L.-M. Chen, X. Lu, J.-L. Ma, X. Wang, and J. Zhang, *Phys. Rev. Lett.* **116**, 205003 (2016).
- [13] A. Gopal, S. Herzer, A. Schmidt, P. Singh, A. Reinhard, W. Ziegler, D. Brommel, A. Karmakar, P. Gibbon, U. Dillner, T. May, H-G. Meyer, and G. G. Paulus, *Phys. Rev. Lett.* **111**, 074802 (2013).
- [14] Z. Jin, H. B. Zhuo, T. Nakazawa, J. H. Shin, S. Wakamatsu, N. Yugami, T. Hosokai, D. B. Zou, M. Y. Yu, Z. M. Sheng, and R. Kodama, *Phys. Rev. E* **94**, 033206 (2016).
- [15] R. Kodama, Y. Sentoku, Z. L. Chen, G. R. Kumar, S. P. Hatchett, Y. Toyama, T. E. Cowan, R. R. Freeman, J. Fuchs, Y. Izawa, M. H. Key, Y. Kitagawa, K. Kondo, T. Matsuoka, H. Nakamura, M. Nakatsutsumi, P. A. Norreys, T. Norimatsu, R. A. Snavely, R. B. Stephens, M. Tampo, K. A. Tanaka, and T. Yabuuchi, *Nature (London)* **432**, 1005 (2004).
- [16] F. N. Beg, E. L. Clark, M. S. Wei, A. E. Dangor, R. G. Evans, A. Gopal, K. L. Lancaster, K. W. D. Ledingham, P. McKenna, P. A. Norreys, M. Tatarakis, M. Zepf, and K. Krushelnick, *Phys. Rev. Lett.* **92**, 095001 (2004).
- [17] K. Quinn, P. A. Wilson, C. A. Cecchetti, B. Ramakrishna, L. Romagnani, G. Sarri, L. Lancia, J. Fuchs, A. Pipahl, T. Toncian, O. Willi, R. J. Clarke, D. Neely, M. Notley, P. Gallegos, D. C. Carroll, M. N. Quinn, X. H. Yuan, P. McKenna, T. V. Liseykina, A. Macchi, and M. Borghesi, *Phys. Rev. Lett.* **102**, 194801 (2009).
- [18] S. Tokita, K. Otani, T. Nishoji, S. Inoue, M. Hashida, and S. Sakabe, *Phys. Rev. Lett.* **106**, 255001 (2011).
- [19] H. Nakajima, S. Tokita, S. Inoue, M. Hashida, and S. Sakabe, *Phys. Rev. Lett.* **110**, 155001 (2013).
- [20] T. Nakamura, S. Kato, H. Nagatomo, and K. Mima, *Phys. Rev. Lett.* **93**, 265002 (2004).
- [21] Y. T. Li, X. H. Yuan, M. H. Xu, Z. Y. Zheng, Z. M. Sheng, M. Chen, Y. Y. Ma, W. X. Liang, Q. Z. Yu, Y. Zhang, F. Liu, Z. H. Wang, Z. Y. Wei, W. Zhao, Z. Jin, and J. Zhang, *Phys. Rev. Lett.* **96**, 165003 (2006).
- [22] H. B. Zhuo, W. Yu, M. Y. Yu, H. Xu, X. Wang, B. F. Shen, Z. M. Sheng, and J. Zhang, *Phys. Rev. E* **79**, 015401(R) (2009).
- [23] H. B. Zhuo, Z. L. Chen, Z. M. Sheng, M. Chen, T. Yabuuchi, M. Tampo, M. Y. Yu, X. H. Yang, C. T. Zhou, K. A. Tanaka, J. Zhang, and R. Kodama, *Phys. Rev. Lett.* **112**, 215003 (2014).
- [24] S. C. Wilks and W. L. Kruer, *IEEE J. Quantum Electron* **33**, 1954 (1997).
- [25] G. S. Smith and Thorsten W. Hertel, *IEEE Antennas Propagation Magazine*, **43**, 49 (2001).
- [26] G. S. Smith, *An Introduction to Classical Electromagnetic Radiation* (Cambridge University Press, New York, 1997).
- [27] G. Goubau, *J. App. Phys.* **21**, 1119 (1950).
- [28] K. Wang and D. M. Mittleman, *Phys. Rev. Lett.* **96**, 157401 (2006).
- [29] G. I. Dudnikova, V. Yu. Bychenkov, A. Maksimchuk, G. Mourou, J. Nees, S. G. Bochkarev, and V. A. Vshivkov, *Phys. Rev. E* **67**, 026416 (2003).